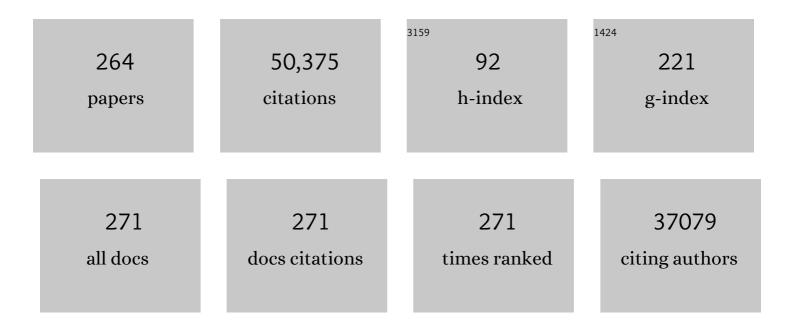
## Daniel G Nocera

List of Publications by Year in descending order

Source: https://exaly.com/author-pdf/26483/publications.pdf Version: 2024-02-01



#	Article	IF	CITATIONS
1	Powering the planet: Chemical challenges in solar energy utilization. Proceedings of the National Academy of Sciences of the United States of America, 2006, 103, 15729-15735.	7.1	7,148
2	In Situ Formation of an Oxygen-Evolving Catalyst in Neutral Water Containing Phosphate and Co <sup>2+</sup> . Science, 2008, 321, 1072-1075.	12.6	3,855
3	Solar Energy Supply and Storage for the Legacy and Nonlegacy Worlds. Chemical Reviews, 2010, 110, 6474-6502.	47.7	2,676
4	Wireless Solar Water Splitting Using Silicon-Based Semiconductors and Earth-Abundant Catalysts. Science, 2011, 334, 645-648.	12.6	1,559
5	The Artificial Leaf. Accounts of Chemical Research, 2012, 45, 767-776.	15.6	1,531
6	Comparing Photosynthetic and Photovoltaic Efficiencies and Recognizing the Potential for Improvement. Science, 2011, 332, 805-809.	12.6	1,369
7	Hydrogen Production by Molecular Photocatalysis. Chemical Reviews, 2007, 107, 4022-4047.	47.7	1,325
8	Mechanistic Studies of the Oxygen Evolution Reaction by a Cobalt-Phosphate Catalyst at Neutral pH. Journal of the American Chemical Society, 2010, 132, 16501-16509.	13.7	1,074
9	Fractionalized excitations in the spin-liquid state of a kagome-lattice antiferromagnet. Nature, 2012, 492, 406-410.	27.8	873
10	PROTON-COUPLED ELECTRON TRANSFER. Annual Review of Physical Chemistry, 1998, 49, 337-369.	10.8	797
11	Radical Initiation in the Class I Ribonucleotide Reductase:  Long-Range Proton-Coupled Electron Transfer?. Chemical Reviews, 2003, 103, 2167-2202.	47.7	770
12	Water splitting–biosynthetic system with CO <sub>2</sub> reduction efficiencies exceeding photosynthesis. Science, 2016, 352, 1210-1213.	12.6	760
13	Nickel-borate oxygen-evolving catalyst that functions under benign conditions. Proceedings of the National Academy of Sciences of the United States of America, 2010, 107, 10337-10341.	7.1	709
14	Cobalt–phosphate oxygen-evolving compound. Chemical Society Reviews, 2009, 38, 109-114.	38.1	683
15	Structure and Valency of a Cobaltâ^'Phosphate Water Oxidation Catalyst Determined by in Situ X-ray Spectroscopy. Journal of the American Chemical Society, 2010, 132, 13692-13701.	13.7	649
16	A Structurally PerfectS=1/2Kagomé Antiferromagnet. Journal of the American Chemical Society, 2005, 127, 13462-13463.	13.7	622
17	Structure–Activity Correlations in a Nickel–Borate Oxygen Evolution Catalyst. Journal of the American Chemical Society, 2012, 134, 6801-6809.	13.7	612
18	Electrolyte-Dependent Electrosynthesis and Activity of Cobalt-Based Water Oxidation Catalysts. Journal of the American Chemical Society, 2009, 131, 2615-2620.	13.7	590

#	Article	IF	CITATIONS
19	A Self-Healing Oxygen-Evolving Catalyst. Journal of the American Chemical Society, 2009, 131, 3838-3839.	13.7	521
20	Quantum spin liquids. Science, 2020, 367, .	12.6	513
21	EPR Evidence for Co(IV) Species Produced During Water Oxidation at Neutral pH. Journal of the American Chemical Society, 2010, 132, 6882-6883.	13.7	488
22	Electocatalytic Water Oxidation by Cobalt(III) Hangman β-Octafluoro Corroles. Journal of the American Chemical Society, 2011, 133, 9178-9180.	13.7	488
23	Influence of iron doping on tetravalent nickel content in catalytic oxygen evolving films. Proceedings of the National Academy of Sciences of the United States of America, 2017, 114, 1486-1491.	7.1	488
24	A Functionally Stable Manganese Oxide Oxygen Evolution Catalyst in Acid. Journal of the American Chemical Society, 2014, 136, 6002-6010.	13.7	474
25	Mechanistic Studies of the Oxygen Evolution Reaction Mediated by a Nickel–Borate Thin Film Electrocatalyst. Journal of the American Chemical Society, 2013, 135, 3662-3674.	13.7	430
26	Proton-Coupled Electron Transfer in Biology: Results from Synergistic Studies in Natural and Model Systems. Annual Review of Biochemistry, 2009, 78, 673-699.	11.1	404
27	Highly active cobalt phosphate and borate based oxygen evolving catalysts operating in neutral and natural waters. Energy and Environmental Science, 2011, 4, 499-504.	30.8	402
28	Electronic Design Criteria for Oâ´'O Bond Formation via Metalâ´'Oxo Complexes. Inorganic Chemistry, 2008, 47, 1849-1861.	4.0	390
29	Quantum-dot optical temperature probes. Applied Physics Letters, 2003, 83, 3555-3557.	3.3	369
30	Chemistry of Personalized Solar Energy. Inorganic Chemistry, 2009, 48, 10001-10017.	4.0	368
31	Efficient solar-to-fuels production from a hybrid microbial–water-splitting catalyst system. Proceedings of the National Academy of Sciences of the United States of America, 2015, 112, 2337-2342.	7.1	366
32	Nature of Activated Manganese Oxide for Oxygen Evolution. Journal of the American Chemical Society, 2015, 137, 14887-14904.	13.7	359
33	Role of Proton-Coupled Electron Transfer in O–O Bond Activation. Accounts of Chemical Research, 2007, 40, 543-553.	15.6	353
34	Solar Fuels and Solar Chemicals Industry. Accounts of Chemical Research, 2017, 50, 616-619.	15.6	333
35	Hydrogen Produced from Hydrohalic Acid Solutions by a Two-Electron Mixed-Valence Photocatalyst. Science, 2001, 293, 1639-1641.	12.6	309
36	Photocatalytic hydrogen production. Chemical Communications, 2011, 47, 9268.	4.1	300

#	Article	IF	CITATIONS
37	Topological Magnon Bands in a Kagome Lattice Ferromagnet. Physical Review Letters, 2015, 115, 147201.	7.8	289
38	The Nature of Lithium Battery Materials under Oxygen Evolution Reaction Conditions. Journal of the American Chemical Society, 2012, 134, 16959-16962.	13.7	287
39	Artificial photosynthesis as a frontier technology for energy sustainability. Energy and Environmental Science, 2013, 6, 1074.	30.8	284
40	Energy and environment policy case for a global project on artificial photosynthesis. Energy and Environmental Science, 2013, 6, 695.	30.8	264
41	Proton-coupled electron transfer: the mechanistic underpinning for radical transport and catalysis in biology. Philosophical Transactions of the Royal Society B: Biological Sciences, 2006, 361, 1351-1364.	4.0	262
42	Ten-percent solar-to-fuel conversion with nonprecious materials. Proceedings of the National Academy of Sciences of the United States of America, 2014, 111, 14057-14061.	7.1	262
43	Templated assembly of photoswitches significantly increases the energy-storage capacity of solar thermal fuels. Nature Chemistry, 2014, 6, 441-447.	13.6	261
44	Hydrogen Generation by Hangman Metalloporphyrins. Journal of the American Chemical Society, 2011, 133, 8775-8777.	13.7	255
45	Light-driven fine chemical production in yeast biohybrids. Science, 2018, 362, 813-816.	12.6	251
46	Photoinduced electron transfer mediated by a hydrogen-bonded interface. Journal of the American Chemical Society, 1992, 114, 4013-4015.	13.7	243
47	Spin chirality on a two-dimensional frustrated lattice. Nature Materials, 2005, 4, 323-328.	27.5	243
48	Oxygen reduction reactivity of cobalt(ii) hangman porphyrins. Chemical Science, 2010, 1, 411.	7.4	225
49	Reversible, Long-Range Radical Transfer in E. coli Class Ia Ribonucleotide Reductase. Accounts of Chemical Research, 2013, 46, 2524-2535.	15.6	223
50	Artificial Photosynthesis at Efficiencies Greatly Exceeding That of Natural Photosynthesis. Accounts of Chemical Research, 2019, 52, 3143-3148.	15.6	222
51	Nucleation, Growth, and Repair of a Cobalt-Based Oxygen Evolving Catalyst. Journal of the American Chemical Society, 2012, 134, 6326-6336.	13.7	216
52	Alternating layer addition approach to CdSe/CdS core/shell quantum dots with near-unity quantum yield and high on-time fractions. Chemical Science, 2012, 3, 2028.	7.4	207
53	Hangman Corroles: Efficient Synthesis and Oxygen Reaction Chemistry. Journal of the American Chemical Society, 2011, 133, 131-140.	13.7	197
54	Light-induced water oxidation at silicon electrodes functionalized with a cobalt oxygen-evolving catalyst. Proceedings of the National Academy of Sciences of the United States of America, 2011, 108, 10056-10061.	7.1	195

#	Article	IF	CITATIONS
55	Proton-Coupled Electron Transfer of Tyrosine Oxidation:  Buffer Dependence and Parallel Mechanisms. Journal of the American Chemical Society, 2007, 129, 15462-15464.	13.7	193
56	Probing Edge Site Reactivity of Oxidic Cobalt Water Oxidation Catalysts. Journal of the American Chemical Society, 2016, 138, 4229-4236.	13.7	178
57	Electrochemical trapping of metastable Mn <sup>3+</sup> ions for activation of MnO <sub>2</sub> oxygen evolution catalysts. Proceedings of the National Academy of Sciences of the United States of America, 2018, 115, E5261-E5268.	7.1	173
58	Design of template-stabilized active and earth-abundant oxygen evolution catalysts in acid. Chemical Science, 2017, 8, 4779-4794.	7.4	172
59	Ambient nitrogen reduction cycle using a hybrid inorganic–biological system. Proceedings of the National Academy of Sciences of the United States of America, 2017, 114, 6450-6455.	7.1	167
60	Site Specific X-ray Anomalous Dispersion of the Geometrically Frustrated Kagomé Magnet, Herbertsmithite, ZnCu <sub>3</sub> (OH) <sub>6</sub> Cl <sub>2</sub> . Journal of the American Chemical Society, 2010, 132, 16185-16190.	13.7	166
61	Role of pendant proton relays and proton-coupled electron transfer on the hydrogen evolution reaction by nickel hangman porphyrins. Proceedings of the National Academy of Sciences of the United States of America, 2014, 111, 15001-15006.	7.1	159
62	Electrochemical polymerization of pyrene derivatives on functionalized carbon nanotubes for pseudocapacitive electrodes. Nature Communications, 2015, 6, 7040.	12.8	159
63	Proton-Coupled Oâ^'O Activation on a Redox Platform Bearing a Hydrogen-Bonding Scaffold. Journal of the American Chemical Society, 2003, 125, 1866-1876.	13.7	158
64	Electronic Structure Description of a [Co(III) <sub>3</sub> Co(IV)O <sub>4</sub> ] Cluster: A Model for the Paramagnetic Intermediate in Cobalt-Catalyzed Water Oxidation. Journal of the American Chemical Society, 2011, 133, 15444-15452.	13.7	155
65	Blue semiconductor nanocrystal laser. Applied Physics Letters, 2005, 86, 073102.	3.3	154
66	Water Oxidation Catalysis by Co(II) Impurities in Co(III) <sub>4</sub> O <sub>4</sub> Cubanes. Journal of the American Chemical Society, 2014, 136, 17681-17688.	13.7	152
67	Proton-coupled electron transfer kinetics for the hydrogen evolution reaction of hangman porphyrins. Energy and Environmental Science, 2012, 5, 7737.	30.8	151
68	Intermediate-Range Structure of Self-Assembled Cobalt-Based Oxygen-Evolving Catalyst. Journal of the American Chemical Society, 2013, 135, 6403-6406.	13.7	151
69	Proton–Electron Transport and Transfer in Electrocatalytic Films. Application to a Cobalt-Based O2-Evolution Catalyst. Journal of the American Chemical Society, 2013, 135, 10492-10502.	13.7	151
70	Photoinduced Electron Transfer within a Donor-Acceptor Pair Juxtaposed by a Salt Bridge. Journal of the American Chemical Society, 1995, 117, 8051-8052.	13.7	148
71	Electrocatalytic four-electron reduction of oxygen to water by a highly flexible cofacial cobalt bisporphyrin. Chemical Communications, 2000, , 1355-1356.	4.1	148
72	Photocatalytic Oxidation of Hydrocarbons by a Bis-iron(III)-μ-oxo Pacman Porphyrin Using O2and Visible Light. Journal of the American Chemical Society, 2006, 128, 6546-6547.	13.7	139

#	Article	IF	CITATIONS
73	Nickel phlorin intermediate formed by proton-coupled electron transfer in hydrogen evolution mechanism. Proceedings of the National Academy of Sciences of the United States of America, 2016, 113, 485-492.	7.1	133
74	"Hangman―Porphyrins for the Assembly of a Model Heme Water Channel. Journal of the American Chemical Society, 2001, 123, 1513-1514.	13.7	129
75	Bidirectional and Unidirectional PCET in a Molecular Model of a Cobalt-Based Oxygen-Evolving Catalyst. Journal of the American Chemical Society, 2011, 133, 5174-5177.	13.7	127
76	Spin Frustration in 2D Kagomé Lattices: A Problem for Inorganic Synthetic Chemistry. Chemistry - A European Journal, 2004, 10, 3850-3859.	3.3	126
77	Mono-, Di-, Tri-, and Tetra-Substituted Fluorotyrosines:Â New Probes for Enzymes That Use Tyrosyl Radicals in Catalysisâ€. Journal of the American Chemical Society, 2006, 128, 1569-1579.	13.7	126
78	Trap-Free Halogen Photoelimination from Mononuclear Ni(III) Complexes. Journal of the American Chemical Society, 2015, 137, 6472-6475.	13.7	125
79	Ribonucleotide Reductases: Structure, Chemistry, and Metabolism Suggest New Therapeutic Targets. Annual Review of Biochemistry, 2020, 89, 45-75.	11.1	120
80	Elucidation of a Redox-Mediated Reaction Cycle for Nickel-Catalyzed Cross Coupling. Journal of the American Chemical Society, 2019, 141, 89-93.	13.7	119
81	pH Rate Profiles of FnY356â^'R2s (n= 2, 3, 4) inEscherichiacoliRibonucleotide Reductase:Â Evidence that Y356Is a Redox-Active Amino Acid along the Radical Propagation Pathway. Journal of the American Chemical Society, 2006, 128, 1562-1568.	13.7	114
82	Halogen Photoreductive Elimination from Gold(III) Centers. Journal of the American Chemical Society, 2009, 131, 7411-7420.	13.7	109
83	Personalized Energy: The Home as a Solar Power Station and Solar Gas Station. ChemSusChem, 2009, 2, 387-390.	6.8	108
84	Carbon Dioxide Reduction by Iron Hangman Porphyrins. Organometallics, 2019, 38, 1219-1223.	2.3	108
85	Xanthene-Bridged Cofacial Bisporphyrins. Inorganic Chemistry, 2000, 39, 959-966.	4.0	107
86	Photo-assisted water oxidation with cobalt-based catalyst formed from thin-film cobalt metal on silicon photoanodes. Energy and Environmental Science, 2011, 4, 2058.	30.8	106
87	Micelle-Encapsulated Quantum Dot-Porphyrin Assemblies as <i>in Vivo</i> Two-Photon Oxygen Sensors. Journal of the American Chemical Society, 2015, 137, 9832-9842.	13.7	104
88	Oxygen and hydrogen photocatalysis by two-electron mixed-valence coordination compounds. Coordination Chemistry Reviews, 2005, 249, 1316-1326.	18.8	103
89	The Whole Story of the Two-Electron Bond, with the $\hat{I}'$ Bond as a Paradigm. Accounts of Chemical Research, 2000, 33, 483-490.	15.6	102
90	Interplay of Homogeneous Reactions, Mass Transport, and Kinetics in Determining Selectivity of the Reduction of CO <sub>2</sub> on Gold Electrodes. ACS Central Science, 2019, 5, 1097-1105.	11.3	97

#	Article	IF	CITATIONS
91	Catalytic Oâ^'O Activation Chemistry Mediated by Iron Hangman Porphyrins with a Wide Range of Proton-Donating Abilities. Organic Letters, 2003, 5, 2421-2424.	4.6	95
92	Self-healing catalysis in water. Proceedings of the National Academy of Sciences of the United States of America, 2017, 114, 13380-13384.	7.1	95
93	X-ray Spectroscopic Characterization of Co(IV) and Metal–Metal Interactions in Co <sub>4</sub> O <sub>4</sub> : Electronic Structure Contributions to the Formation of High-Valent States Relevant to the Oxygen Evolution Reaction. Journal of the American Chemical Society, 2016, 138, 11017-11030.	13.7	94
94	In situ characterization of cofacial Co(IV) centers in Co <sub>4</sub> O <sub>4</sub> cubane: Modeling the high-valent active site in oxygen-evolving catalysts. Proceedings of the National Academy of Sciences of the United States of America, 2017, 114, 3855-3860.	7.1	93
95	Proton-Directed Redox Control of Oâ^'O Bond Activation by Heme Hydroperoxidase Models. Journal of the American Chemical Society, 2007, 129, 5069-5075.	13.7	91
96	Oxygen Reduction Reaction Promoted by Manganese Porphyrins. ACS Catalysis, 2018, 8, 8671-8679.	11.2	91
97	Theoretical Analysis of Cobalt Hangman Porphyrins: Ligand Dearomatization and Mechanistic Implications for Hydrogen Evolution. ACS Catalysis, 2014, 4, 4516-4526.	11.2	90
98	Reversible Reduction of Oxygen to Peroxide Facilitated by Molecular Recognition. Science, 2012, 335, 450-453.	12.6	87
99	Oxygen Reduction Catalysis at a Dicobalt Center: The Relationship of Faradaic Efficiency to Overpotential. Journal of the American Chemical Society, 2016, 138, 2925-2928.	13.7	84
100	General Paradigm in Photoredox Nickel atalyzed Crossâ€Coupling Allows for Lightâ€Free Access to Reactivity. Angewandte Chemie - International Edition, 2020, 59, 9527-9533.	13.8	84
101	Electrocatalytic H <sub>2</sub> Evolution by Proton-Gated Hangman Iron Porphyrins. Organometallics, 2014, 33, 4994-5001.	2.3	82
102	Spectroscopic Determination of Proton Position in the Proton-Coupled Electron Transfer Pathways of Donorâ <sup>~</sup> Acceptor Supramolecule Assemblies. Journal of the American Chemical Society, 2006, 128, 10474-10483.	13.7	81
103	Generation of the R2 Subunit of Ribonucleotide Reductase by Intein Chemistry:Â Insertion of 3-Nitrotyrosine at Residue 356 as a Probe of the Radical Initiation Processâ€. Biochemistry, 2003, 42, 14541-14552.	2.5	79
104	A ligand field chemistry of oxygen generation by the oxygen-evolving complex and synthetic active sites. Philosophical Transactions of the Royal Society B: Biological Sciences, 2008, 363, 1293-1303.	4.0	79
105	Two-Photon Oxygen Sensing with Quantum Dot-Porphyrin Conjugates. Inorganic Chemistry, 2013, 52, 10394-10406.	4.0	76
106	Electronic Structure of Copper Corroles. Angewandte Chemie - International Edition, 2016, 55, 2176-2180.	13.8	76
107	xmlns:mml="http://www.w3.org/1998/Math/MathML" display="inline"> <mml:mrow><mml:mfrac><mml:mrow><mml:mn>1</mml:mn></mml:mrow><mml:mrow><n antiferromagnets Zn<mml:math <br="" xmlns:mml="http://www.w3.org/1998/Math/MathML">display="inline"&gt;<mml:mrow><mml:msub><mml:mrow< td=""><td>nml:mn&gt;2&lt;</td><td>/mml;mn&gt;</td></mml:mrow<></mml:msub></mml:mrow></mml:math></n </mml:mrow></mml:mfrac></mml:mrow>	nml:mn>2<	/mml;mn>
108	/> <mml:mrow> <mml:mi> </mml:mi> </mml:mrow> <td>3.2</td> <td>73</td>	3.2	73

#	Article	IF	CITATIONS
109	Nucleation and Growth Mechanisms of an Electrodeposited Manganese Oxide Oxygen Evolution Catalyst. Journal of Physical Chemistry C, 2014, 118, 17142-17152.	3.1	73
110	Halogen Photoelimination from Monomeric Nickel(III) Complexes Enabled by the Secondary Coordination Sphere. Organometallics, 2015, 34, 4766-4774.	2.3	73
111	Proton-Coupled Electron Transfer: The Engine of Energy Conversion and Storage. Journal of the American Chemical Society, 2022, 144, 1069-1081.	13.7	72
112	Catalase and Epoxidation Activity of Manganese Salen Complexes Bearing Two Xanthene Scaffolds. Journal of the American Chemical Society, 2007, 129, 8192-8198.	13.7	66
113	Chlorine Photoelimination from a Diplatinum Core: Circumventing the Back Reaction. Journal of the American Chemical Society, 2009, 131, 28-29.	13.7	66
114	Excited-State Dynamics of Cofacial Pacman Porphyrins. Journal of Physical Chemistry A, 2002, 106, 11700-11708.	2.5	65
115	Room temperature stable CO <sub> <i>x</i> </sub> -free H <sub>2</sub> production from methanol with magnesium oxide nanophotocatalysts. Science Advances, 2016, 2, e1501425.	10.3	62
116	Taming the Chlorine Radical: Enforcing Steric Control over Chlorine-Radical-Mediated C–H Activation. Journal of the American Chemical Society, 2022, 144, 1464-1472.	13.7	62
117	From Molecules to the Crystalline Solid: Secondary Hydrogen-Bonding Interactions of Salt Bridges and Their Role in Magnetic Exchange. Chemistry - A European Journal, 1999, 5, 1474-1480.	3.3	61
118	General Strategy for Improving the Quantum Efficiency of Photoredox Hydroamidation Catalysis. Journal of the American Chemical Society, 2018, 140, 14926-14937.	13.7	61
119	Photoredox Nickel-Catalyzed C–S Cross-Coupling: Mechanism, Kinetics, and Generalization. Journal of the American Chemical Society, 2021, 143, 2005-2015.	13.7	61
120	2,3-Difluorotyrosine at Position 356 of Ribonucleotide Reductase R2:  A Probe of Long-Range Proton-Coupled Electron Transfer. Journal of the American Chemical Society, 2003, 125, 10506-10507.	13.7	60
121	A nanocrystal-based ratiometric pH sensor for natural pH ranges. Chemical Science, 2012, 3, 2980.	7.4	60
122	Valorization of CO2 through lithoautotrophic production of sustainable chemicals in Cupriavidus necator. Metabolic Engineering, 2020, 62, 207-220.	7.0	60
123	On the future of global energy. Daedalus, 2006, 135, 112-115.	1.8	59
124	Direct formation of a water oxidation catalyst from thin-film cobalt. Energy and Environmental Science, 2010, 3, 1726.	30.8	59
125	Interfaces between water splitting catalysts and buried silicon junctions. Energy and Environmental Science, 2013, 6, 532-538.	30.8	58
126	Proton-coupled electron transfer chemistry of hangman macrocycles: Hydrogen and oxygen evolution reactions. Journal of Porphyrins and Phthalocyanines, 2015, 19, 1-8.	0.8	58

#	Article	IF	CITATIONS
127	Practical challenges in the development of photoelectrochemical solar fuels production. Sustainable Energy and Fuels, 2020, 4, 985-995.	4.9	58
128	Hydrogen Evolution Catalysis by a Sparsely Substituted Cobalt Chlorin. ACS Catalysis, 2017, 7, 3597-3606.	11.2	56
129	Porphyrin Architectures Bearing Functionalized Xanthene Spacers. Journal of Organic Chemistry, 2002, 67, 1403-1406.	3.2	54
130	Transient Absorption Studies of the Pacman Effect in Spring-Loaded Diiron(III) μ-Oxo Bisporphyrins. Inorganic Chemistry, 2003, 42, 8270-8277.	4.0	54
131	Exciton-exciton annihilation in organic polariton microcavities. Physical Review B, 2010, 82, .	3.2	54
132	Photo-ribonucleotide reductase β2 by selective cysteine labeling with a radical phototrigger. Proceedings of the National Academy of Sciences of the United States of America, 2012, 109, 39-43.	7.1	53
133	How Radical Are "Radical―Photocatalysts? A Closed-Shell Meisenheimer Complex Is Identified as a Super-Reducing Photoreagent. Journal of the American Chemical Society, 2021, 143, 14352-14359.	13.7	53
134	Xanthene-Modified and Hangman Iron Corroles. Inorganic Chemistry, 2011, 50, 1368-1377.	4.0	52
135	Dzyaloshinskii-Moriya interaction and spin reorientation transition in the frustrated kagome lattice antiferromagnet. Physical Review B, 2011, 83, .	3.2	50
136	Electrochemical Deposition of Conformal and Functional Layers on High Aspect Ratio Silicon Micro/Nanowires. Nano Letters, 2017, 17, 4502-4507.	9.1	50
137	Activation of Electronâ€Deficient Quinones through Hydrogenâ€Bondâ€Donorâ€Coupled Electron Transfer. Angewandte Chemie - International Edition, 2016, 55, 539-544.	13.8	49
138	Efficient Synthesis of Hangman Porphyrins. Organic Letters, 2010, 12, 1036-1039.	4.6	48
139	Tertiary Amine-Assisted Electroreduction of Carbon Dioxide to Formate Catalyzed by Iron Tetraphenylporphyrin. ACS Energy Letters, 2020, 5, 72-78.	17.4	48
140	Long-Lived Triplet Excited State in a Heterogeneous Modified Carbon Nitride Photocatalyst. Journal of the American Chemical Society, 2021, 143, 4646-4652.	13.7	48
141	Photophysical Properties of Î <sup>2</sup> -Substituted Free-Base Corroles. Inorganic Chemistry, 2015, 54, 2713-2725.	4.0	47
142	Solar-driven tandem photoredox nickel-catalysed cross-coupling using modified carbon nitride. Chemical Science, 2020, 11, 7456-7461.	7.4	47
143	Catalytic Oxygen Evolution by Cobalt Oxido Thin Films. Topics in Current Chemistry, 2015, 371, 173-213.	4.0	46
144	Slow Magnetic Relaxation in Intermediate Spin <i>S</i> = 3/2 Mononuclear Fe(III) Complexes. Journal of the American Chemical Society, 2017, 139, 16474-16477.	13.7	46

#	Article	IF	CITATIONS
145	Self-healing oxygen evolution catalysts. Nature Communications, 2022, 13, 1243.	12.8	46
146	Stereochemical control of H2O2 dismutation by Hangman porphyrins. Chemical Communications, 2007, , 2642.	4.1	44
147	Photoactive Peptides for Light-Initiated Tyrosyl Radical Generation and Transport into Ribonucleotide Reductase. Journal of the American Chemical Society, 2007, 129, 8500-8509.	13.7	44
148	Generation of a stable, aminotyrosyl radical-induced α2β2 complex of <i>Escherichia coli</i> class Ia ribonucleotide reductase. Proceedings of the National Academy of Sciences of the United States of America, 2013, 110, 3835-3840.	7.1	44
149	Continuous electrochemical water splitting from natural water sources via forward osmosis. Proceedings of the National Academy of Sciences of the United States of America, 2021, 118, .	7.1	44
150	Gold Corroles as Near-IR Phosphors for Oxygen Sensing. Inorganic Chemistry, 2017, 56, 10991-10997.	4.0	43
151	Double Hangman Iron Porphyrin and the Effect of Electrostatic Nonbonding Interactions on Carbon Dioxide Reduction. Journal of Physical Chemistry Letters, 2020, 11, 1890-1895.	4.6	42
152	Template-stabilized oxidic nickel oxygen evolution catalysts. Proceedings of the National Academy of Sciences of the United States of America, 2020, 117, 16187-16192.	7.1	41
153	Deciphering Radical Transport in the Large Subunit of Class I Ribonucleotide Reductase. Journal of the American Chemical Society, 2012, 134, 1172-1180.	13.7	40
154	Proton–Electron Conductivity in Thin Films of a Cobalt–Oxygen Evolving Catalyst. ACS Applied Energy Materials, 2019, 2, 3-12.	5.1	39
155	Detection of high-valent iron species in alloyed oxidic cobaltates for catalysing the oxygen evolution reaction. Nature Communications, 2021, 12, 4218.	12.8	38
156	Can We Progress from Solipsistic Science to Frugal Innovation?. Daedalus, 2012, 141, 45-52.	1.8	37
157	Photocatalytic Hydromethylation and Hydroalkylation of Olefins Enabled by Titanium Dioxide Mediated Decarboxylation. Journal of the American Chemical Society, 2020, 142, 17913-17918.	13.7	37
158	Pseudotetrahedral d0, d1, and d2Metalâ^'Oxo Cores within a Tris(alkoxide) Platform. Inorganic Chemistry, 2010, 49, 10759-10761.	4.0	36
159	"Fast food―energy. Energy and Environmental Science, 2010, 3, 993.	30.8	36
160	Mechanism of Cobalt Self-Exchange Electron Transfer. Journal of the American Chemical Society, 2013, 135, 15053-15061.	13.7	36
161	Conformationally Dynamic Radical Transfer within Ribonucleotide Reductase. Journal of the American Chemical Society, 2017, 139, 16657-16665.	13.7	36
162	Biological-inorganic hybrid systems as a generalized platform for chemical production. Current Opinion in Chemical Biology, 2017, 41, 107-113.	6.1	36

#	Article	IF	CITATIONS
163	Hangman Salen Platforms Containing Two Xanthene Scaffolds. Journal of Organic Chemistry, 2006, 71, 8706-8714.	3.2	35
164	Halogen photoelimination from dirhodium phosphazane complexes via chloride-bridged intermediates. Chemical Science, 2013, 4, 2880.	7.4	35
165	Formal Reduction Potentials of Difluorotyrosine and Trifluorotyrosine Protein Residues: Defining the Thermodynamics of Multistep Radical Transfer. Journal of the American Chemical Society, 2017, 139, 2994-3004.	13.7	34
166	Direct Electrochemical P(V) to P(III) Reduction of Phosphine Oxide Facilitated by Triaryl Borates. Journal of the American Chemical Society, 2018, 140, 13711-13718.	13.7	34
167	Spectroscopic Studies of Nanoparticulate Thin Films of a Cobalt-Based Oxygen Evolution Catalyst. Journal of Physical Chemistry C, 2014, 118, 17060-17066.	3.1	33
168	Hangman effect on hydrogen peroxide dismutation by Fe(iii) corroles. Chemical Communications, 2012, 48, 4175.	4.1	32
169	Kinetics of Hydrogen Atom Abstraction from Substrate by an Active Site Thiyl Radical in Ribonucleotide Reductase. Journal of the American Chemical Society, 2014, 136, 16210-16216.	13.7	32
170	Ligand Noninnocence in Nickel Porphyrins: Nickel Isobacteriochlorin Formation under Hydrogen Evolution Conditions. Inorganic Chemistry, 2019, 58, 7958-7968.	4.0	32
171	Halide-Bridged Binuclear HX-Splitting Catalysts. Inorganic Chemistry, 2014, 53, 9122-9128.	4.0	31
172	General Paradigm in Photoredox Nickelâ€Catalyzed Crossâ€Coupling Allows for Lightâ€Free Access to Reactivity. Angewandte Chemie, 2020, 132, 9614-9620.	2.0	31
173	Family of Cofacial Bimetallic Complexes of a Hexaanionic Carboxamide Cryptand. Inorganic Chemistry, 2011, 50, 4107-4115.	4.0	30
174	Iron in a Trigonal Tris(alkoxide) Ligand Environment. Inorganic Chemistry, 2013, 52, 3159-3169.	4.0	30
175	On the incompatibility of lithium–O <sub>2</sub> battery technology with CO <sub>2</sub> . Chemical Science, 2017, 8, 6117-6122.	7.4	30
176	Solar-powered CO2 reduction by a hybrid biological   inorganic system. Journal of Photochemistry and Photobiology A: Chemistry, 2018, 358, 411-415.	3.9	29
177	Hydrothermal growth of single crystals of the quantum magnets: Clinoatacamite, paratacamite, and herbertsmithite. Applied Physics Letters, 2011, 98, .	3.3	28
178	Charge-Transfer Dynamics at the α/β Subunit Interface of a Photochemical Ribonucleotide Reductase. Journal of the American Chemical Society, 2016, 138, 1196-1205.	13.7	28
179	Halogen Photoelimination from Sb <sup>V</sup> Dihalide Corroles. Inorganic Chemistry, 2018, 57, 5333-5342.	4.0	28
180	Structurally characterized terminal manganese( <scp>iv</scp> ) oxo tris(alkoxide) complex. Chemical Science, 2018, 9, 4524-4528.	7.4	28

#	Article	IF	CITATIONS
181	Bacterial Phosphate Granules Contain Cyclic Polyphosphates: Evidence from <sup>31</sup> P Solid-State NMR. Journal of the American Chemical Society, 2020, 142, 18407-18421.	13.7	28
182	Mechanistic Investigation and Optimization of Photoredox Anti-Markovnikov Hydroamination. Journal of the American Chemical Society, 2021, 143, 10232-10242.	13.7	28
183	A >200 meV Uphill Thermodynamic Landscape for Radical Transport in <i>Escherichia coli</i> Ribonucleotide Reductase Determined Using Fluorotyrosine-Substituted Enzymes. Journal of the American Chemical Society, 2016, 138, 13706-13716.	13.7	27
184	Anion-Receptor Mediated Oxidation of Carbon Monoxide to Carbonate by Peroxide Dianion. Journal of the American Chemical Society, 2015, 137, 14562-14565.	13.7	26
185	Electronic Structure of Copper Corroles. Angewandte Chemie, 2016, 128, 2216-2220.	2.0	26
186	Selective Production of Oxygen from Seawater by Oxidic Metallate Catalysts. ACS Omega, 2019, 4, 12860-12864.	3.5	26
187	Impactful Role of Cocatalysts on Molecular Electrocatalytic Hydrogen Production. ACS Catalysis, 2021, 11, 4561-4567.	11.2	26
188	Structurally Homologousl <sup>2</sup> - andmeso-Amidinium Porphyrins. Inorganic Chemistry, 2001, 40, 3643-3646.	4.0	25
189	Magnetic transitions in the topological magnon insulator Cu(1,3-bdc). Physical Review B, 2016, 93, .	3.2	25
190	Multielectron, multisubstrate molecular catalysis of electrochemical reactions: Formal kinetic analysis in the total catalysis regime. Proceedings of the National Academy of Sciences of the United States of America, 2017, 114, 11303-11308.	7.1	24
191	Powder neutron diffraction analysis and magnetic structure of kagomé-type vanadium jarositeNaV3(OD)6(SO4)2. Physical Review B, 2003, 68, .	3.2	23
192	Chromium(IV) Siloxide. Inorganic Chemistry, 2013, 52, 1173-1175.	4.0	23
193	Radicals in Biology: Your Life Is in Their Hands. Journal of the American Chemical Society, 2021, 143, 13463-13472.	13.7	23
194	Two Photon Excitation Spectrum of a Twisted Quadruple Bond Metalâ^'Metal Complex. Journal of the American Chemical Society, 1999, 121, 868-869.	13.7	22
195	Cofacial Dicobalt Complex of a Binucleating Hexacarboxamide Cryptand Ligand. Inorganic Chemistry, 2010, 49, 3697-3699.	4.0	22
196	Reverse Electron Transfer Completes the Catalytic Cycle in a 2,3,5-Trifluorotyrosine-Substituted Ribonucleotide Reductase. Journal of the American Chemical Society, 2015, 137, 14387-14395.	13.7	22
197	Stereoelectronic Effects in Cl <sub>2</sub> Elimination from Binuclear Pt(III) Complexes. Inorganic Chemistry, 2016, 55, 11815-11820.	4.0	22
198	Capturing the Complete Reaction Profile of a C–H Bond Activation. Journal of the American Chemical Society, 2021, 143, 6060-6064.	13.7	21

#	Article	IF	CITATIONS
199	Catalytic C(β)–O Bond Cleavage of Lignin in a One-Step Reaction Enabled by a Spin-Center Shift. ACS Catalysis, 2021, 11, 14181-14187.	11.2	21
200	Non-linear transduction strategies for chemo/biosensing on small length scales. Journal of Materials Chemistry, 2005, 15, 2697.	6.7	20
201	Stabilized CdSe-CoPi Composite Photoanode for Light-Assisted Water Oxidation by Transformation of a CdSe/Cobalt Metal Thin Film. ACS Applied Materials & amp; Interfaces, 2013, 5, 2364-2367.	8.0	20
202	Activation of Electronâ€Deficient Quinones through Hydrogenâ€Bondâ€Donorâ€Coupled Electron Transfer. Angewandte Chemie, 2016, 128, 549-554.	2.0	20
203	Second-Coordination-Sphere Assisted Selective Colorimetric Turn-on Fluoride Sensing by a Mono-Metallic Co(II) Hexacarboxamide Cryptand Complex. Inorganic Chemistry, 2017, 56, 7615-7619.	4.0	20
204	On the Conversion Efficiency of CO2 Electroreduction on Gold. Joule, 2019, 3, 1565-1568.	24.0	20
205	Dual-Phase Molecular-like Charge Transport in Nanoporous Transition Metal Oxides. Journal of Physical Chemistry C, 2019, 123, 1966-1973.	3.1	20
206	Glutamate 350 Plays an Essential Role in Conformational Gating of Long-Range Radical Transport in <i>Escherichia coli</i> Class Ia Ribonucleotide Reductase. Biochemistry, 2017, 56, 856-868.	2.5	19
207	Direct Seawater Splitting by Forward Osmosis Coupled to Water Electrolysis. ACS Applied Energy Materials, 2022, 5, 1403-1408.	5.1	18
208	Comparison of self-assembled and micelle encapsulated QD chemosensor constructs for biological sensing. Faraday Discussions, 2015, 185, 249-266.	3.2	17
209	Porphyrin and Corrole Platforms for Water Oxidation, Oxygen Reduction, and Peroxide Dismutation. Handbook of Porphyrin Science, 2012, , 1-143.	0.8	16
210	Modulation of Y <sub>356</sub> Photooxidation in <i>E. coli</i> Class la Ribonucleotide Reductase by Y <sub>731</sub> Across the α <sub>2</sub> :β <sub>2</sub> Interface. Journal of the American Chemical Society, 2013, 135, 13250-13253.	13.7	16
211	Tandem redox mediator/Ni( <scp>ii</scp> ) trihalide complex photocycle for hydrogen evolution from HCl. Chemical Science, 2015, 6, 917-922.	7.4	16
212	Energy catalysis needs ligands with high oxidative stability. Chem Catalysis, 2021, 1, 32-43.	6.1	16
213	Energy transfer of CdSe/ZnS nanocrystals encapsulated with rhodamine-dye functionalized poly(acrylic acid). Journal of Photochemistry and Photobiology A: Chemistry, 2012, 248, 24-29.	3.9	15
214	Pacman and Hangman Metal Tetraazamacrocycles. ChemSusChem, 2013, 6, 1541-1544.	6.8	15
215	Experimental evidence of diffusion-induced bias in near-wall velocimetry using quantum dot measurements. Experiments in Fluids, 2008, 44, 1035-1038.	2.4	14
216	Photochemical Generation of a Tryptophan Radical within the Subunit Interface of Ribonucleotide Reductase. Biochemistry, 2016, 55, 3234-3240.	2.5	14

#	Article	IF	CITATIONS
217	Multielectron C–H photoactivation with an Sb(v) oxo corrole. Chemical Communications, 2020, 56, 5247-5250.	4.1	14
218	Gated Proton Release during Radical Transfer at the Subunit Interface of Ribonucleotide Reductase. Journal of the American Chemical Society, 2021, 143, 176-183.	13.7	14
219	Role of electrolyte composition on the acid stability of mixed-metal oxygen evolution catalysts. Chemical Communications, 2020, 56, 10477-10480.	4.1	13
220	Electronic thermal transport measurement in low-dimensional materials with graphene non-local noise thermometry. Nature Nanotechnology, 2022, 17, 166-173.	31.5	13
221	Ultrafast Photoinduced Electron Transfer from Peroxide Dianion. Journal of Physical Chemistry B, 2015, 119, 7422-7429.	2.6	12
222	Scalable Syntheses of 4-Substituted Pyridine–Diimines. Journal of Organic Chemistry, 2017, 82, 12933-12938.	3.2	12
223	Properties of Site-Specifically Incorporated 3-Aminotyrosine in Proteins To Study Redox-Active Tyrosines: <i>Escherichia coli</i> Ribonucleotide Reductase as a Paradigm. Biochemistry, 2018, 57, 3402-3415.	2.5	12
224	Multi-electron reactivity of a cofacial di-tin( <scp>ii</scp> ) cryptand: partial reduction of sulfur and selenium and reversible generation of S <sub>3</sub> E™ <sup>â^'</sup> . Chemical Science, 2016, 7, 6928-6933.	7.4	11
225	13C-Labeling the carbon-fixation pathway of a highly efficient artificial photosynthetic system. Faraday Discussions, 2017, 198, 529-537.	3.2	11
226	Photochemical Rescue of a Conformationally Inactivated Ribonucleotide Reductase. Journal of the American Chemical Society, 2018, 140, 15744-15752.	13.7	11
227	High-Frequency and -Field EPR (HFEPR) Investigation of a Pseudotetrahedral Cr <sup>IV</sup> Siloxide Complex and Computational Studies of Related Cr <sup>IV</sup> L <sub>4</sub> Systems. Inorganic Chemistry, 2019, 58, 4907-4920.	4.0	11
228	Selenocysteine Substitution in a Class I Ribonucleotide Reductase. Biochemistry, 2019, 58, 5074-5084.	2.5	11
229	Driving force dependence of inner-sphere electron transfer for the reduction of CO2 on a gold electrode. Journal of Chemical Physics, 2020, 153, 094701.	3.0	11
230	Modulation of Phenol Oxidation in Cofacial Dyads. Journal of the American Chemical Society, 2015, 137, 11860-11863.	13.7	10
231	Subunit Interaction Dynamics of Class Ia Ribonucleotide Reductases: In Search of a Robust Assay. Biochemistry, 2020, 59, 1442-1453.	2.5	10
232	Cascade Electrochemical Reduction of Carbon Dioxide with Bimetallic Nanowire and Foam Electrodes. ChemElectroChem, 2021, 8, 1918-1924.	3.4	10
233	Die Amidinium arboxylat‧alzbrücke als Protonenübertragungsschnittstelle für Elektronentransferpfade. Angewandte Chemie, 1997, 109, 2216-2219.	2.0	9
234	Oxygen Reduction Mechanism of Monometallic Rhodium Hydride Complexes. Inorganic Chemistry, 2015, 54, 7335-7344.	4.0	9

#	Article	IF	CITATIONS
235	High-throughput patterning of photonic structures with tunable periodicity. Proceedings of the National Academy of Sciences of the United States of America, 2015, 112, 5309-5313.	7.1	9
236	Pushing Single-Oxygen-Atom-Bridged Bimetallic Systems to the Right: A Cryptand-Encapsulated Co–O–Co Unit. Journal of the American Chemical Society, 2015, 137, 15354-15357.	13.7	9
237	Oxygen activation at a dicobalt centre of a dipyridylethane naphthyridine complex. Dalton Transactions, 2018, 47, 11903-11908.	3.3	9
238	The Relation between Hydrogen Atom Transfer and Proton-coupled Electron Transfer in Model Systems. , 0, , 503-562.		8
239	Energy transfer mediated by asymmetric hydrogen-bonded interfaces. Chemical Science, 2012, 3, 455-459.	7.4	8
240	Direct interfacial Y <sub>731</sub> oxidation in α <sub>2</sub> by a photoβ <sub>2</sub> subunit of E. coli class la ribonucleotide reductase. Chemical Science, 2015, 6, 4519-4524.	7.4	8
241	Oxidative Degradation of Multi-Carbon Substrates by an Oxidic Cobalt Phosphate Catalyst. Organometallics, 2019, 38, 1200-1203.	2.3	8
242	Hybrid Inorganic-Biological Systems: Faradaic and Quantum Efficiency, Necessary but Not Sufficient. Joule, 2020, 4, 2051-2055.	24.0	8
243	Synthesis of Hangman Chlorins. Journal of Organic Chemistry, 2020, 85, 5065-5072.	3.2	8
244	p-Block Metal Oxide Noninnocence in the Oxygen Evolution Reaction in Acid: The Case of Bismuth Oxide. Chemistry of Materials, 2022, 34, 826-835.	6.7	8
245	Synthesis, Characterization, and Hydrogen Evolution Activity of Metallo- <i>meso</i> -(4-fluoro-2,6-dimethylphenyl)porphyrin Derivatives. ACS Omega, 2022, 7, 8988-8994.	3.5	8
246	Postâ€ <b>S</b> ynthetic Modification of Hangman Porphyrins Synthesized on the Gram Scale. ChemSusChem, 2014, 7, 2449-2452.	6.8	7
247	Influence of the proton relay spacer on hydrogen electrocatalysis by cobalt hangman porphyrins. Journal of Porphyrins and Phthalocyanines, 2021, 25, 714-723.	0.8	7
248	Basis of dATP inhibition of RNRs. Journal of Biological Chemistry, 2018, 293, 10413-10414.	3.4	6
249	Direct Observation of Different One- and Two-Photon Fluorescent States in a Pyrrolo[3,2- <i>b</i> )pyrrole Fluorophore. Journal of Physical Chemistry Letters, 2020, 11, 4866-4872.	4.6	6
250	Proton-coupled electron transfer of macrocyclic ring hydrogenation: The chlorinphlorin. Proceedings of the National Academy of Sciences of the United States of America, 2022, 119, e2122063119.	7.1	6
251	Facile, Rapid, and Large-Area Periodic Patterning of Semiconductor Substrates with Submicron Inorganic Structures. Journal of the American Chemical Society, 2015, 137, 3739-3742.	13.7	5
252	Organometallic and Coordination Complexes. Inorganic Syntheses, 2004, , 49-95.	0.3	3

#	Article	IF	CITATIONS
253	Mechanistic Study for Facile Electrochemical Patterning of Surfaces with Metal Oxides. ACS Nano, 2016, 10, 5321-5325.	14.6	3
254	Polypyrrole-Silicon Nanowire Arrays for Controlled Intracellular Cargo Delivery. Nano Letters, 2022, 22, 366-371.	9.1	3
255	Chemical Challenges that the Peroxide Dianion Presents to Rechargeable Lithium–Air Batteries. Chemistry of Materials, 2022, 34, 3883-3892.	6.7	3
256	High-Field Magnetism of the S=5/2 Kagome-Lattice Antiferromagnet KFe3(OH)6(SO4)2 for the Magnetic Field in the Kagome-Plane. Journal of Low Temperature Physics, 2013, 170, 242-247.	1.4	2
257	EPR Spectroscopic Characterization of a Jahnâ€Teller Distorted ( C 3 v → C s ) Four oordinate Chromium(V) Oxo Species. Israel Journal of Chemistry, 2016, 56, 864-871.	2.3	2
258	Syntheses and solid-state structures of two cofacial (bis)dipyrrin dichromium complexes in different charge states. Acta Crystallographica Section C, Structural Chemistry, 2021, 77, 161-166.	0.5	2
259	Chapter 8. Hybrid Biological–Inorganic Systems for CO2 Conversion to Fuels. RSC Energy and Environment Series, 2020, , 317-346.	0.5	2
260	Ion-pair effects in photoredox chemistry. CheM, 2022, 8, 1796-1799.	11.7	2
261	Photohalogen elimination chemistry in low-valent binuclear nickel complexes. Polyhedron, 2021, 203, 115228.	2.2	1
262	Crystal structure of the RuPhos ligand. Acta Crystallographica Section E: Crystallographic Communications, 2021, 77, 171-174.	0.5	1
263	Lithium superoxide encapsulated in a benzoquinone anion matrix. Proceedings of the National Academy of Sciences of the United States of America, 2021, 118, .	7.1	1
264	Lithographyâ€Free Electrochemical Patterning of Conductive Substrates with Metal Oxides. Small, 2018, 14, 1801134.	10.0	0